Appl. Phys. B 69, 113–117 (1999) / Digital Object Identifier (DOI) 10.1007/s003409900020

Applied Physics B
Lasers
and Optics

Steering one-dimensional odd dark beams of finite length

A. Dreischuh[1,*], **G.G. Paulus**[1], **F. Zacher**[1], **I. Velchev**[2]

[1] MPI für Quantenoptik, Hans-Kopfermann-Str. 1, D-85748 Garching, Germany
(Fax: +49-89/329-050, E-mail: ggp@mpq.mpg.de)
[2] Vrije Universiteit, Faculteit der Natuurkunde en Sterrenkunde, De Boeleaan 1081, NL-1081 HV Amsterdam, Netherlands
(Fax:+31-20/444-7899, E-mail: iavor@nat.vu.nl)

Received: 26 October 1998/Revised version: 19 January 1999/Published online: 12 May 1999

Abstract. This paper presents arguments for the existence and dynamics of one-dimensional odd dark beams of finite length in bulk Kerr nonlinear media. Their characteristic mixed edge–screw phase dislocations force them to steer in space. The modulational stability of these dark beams and one possible interaction scheme are discussed.

PACS: 42.65; 42.65.Tg; 42.65.Sf

Optical wavefronts can contain dislocations along which the phase is indeterminate and the field amplitude is zero. This concept, introduced in the wave theory by Nye and Berry [1], has allowed clarification of the structure and properties of edge, screw, and mixed edge–screw dislocations. In self-defocusing nonlinear media (or under self-focusing conditions and normal group-velocity dispersion) dark one-dimensional (1D) temporal [2–4], spatial [5, 6] and 2D spatial optical vortex solitons (OVSs) are generated [7–9]. Characteristic of their phase portraits are the transverse (in time or space) 1D π-phase jumps and the on-axis 2π helical phase ramps yielding π-phase jumps in each diametrical cross-section of the OVSs, respectively. The only indication of the existence of mixed edge–screw optical dislocations was found [10] at two interacting vortices of opposite topological charges. Instead of annihilation, a curved zero-intensity line was born in the far-field, crossing the background beam. An extended overview of the physics and potential applications of dark solitons was recently published by Kivshar and Luther-Davies [11].

Inspired by the recent experimental results on the formation of mixed edge–screw phase dislocations [12], we report here extended numerical simulations on the formation and dynamics of one-dimensional odd dark beams (1D ODBs) of finite length in bulk Kerr nonlinear media. The phase portraits of such solitary waves consist of pairs of opposite semi-helices with a phase difference of π. The spatial offset of the semi-helices determines the finite length of the dark stripe. In the direction perpendicular to a line connecting the semi-helices this ensures a π-phase jump (i.e. the odd initial conditions desired). The soliton-like nature of the formation is proved by analyzing the reproducibility of the 1D amplitude and phase distributions across the background beam, which is of finite extent, and by the existence of a constant identical to the soliton constant in the pure 1D case. An inherent feature of the 1D ODBs of finite extent resulting from their phase profiles is their steering, which produces a ‘gray’ final evolution state. Unfortunately the odd dark beams analyzed could not be classified as solitons in the sense of Zabusky and Kruskal [13], since they do not survive after collision with a second ODB of the same length which steers in the opposite direction. In this case the simulations carried out revealed the creation of ring dark solitary waves [14–16]. Along with the data on the stability of the 1D ODBs of finite length we show that multiples of them could be simultaneously incorporated and controllably steered on a common background beam. The latter seems attractive for future parallel all-optical switching applications.

1 Initial conditions and numerical procedure

Generally, the $(2+1)$-dimensional evolution of an optical beam in a bulk homogeneous and isotropic nonlinear medium (NLM) is described by the nonlinear Schrödinger equation

$$\mathrm{i}\frac{\partial E}{\partial \zeta} + (1/2)\left(\frac{\partial^2}{\partial \xi^2} + (a/b)^2\,\frac{\partial^2}{\partial \eta^2}\right)E - \frac{L_{\mathrm{Diff}}}{L_{\mathrm{NL}}}|E|^2 E = 0\,. \quad (1)$$

For convenience, we used the transverse coordinates normalized to the initial dark-beam widths ($\zeta = x/a$, $\eta = y/b$). The nonlinear propagation path length z is expressed in Rayleigh diffraction lengths $L_{\mathrm{Diff}} = ka^2$. The coordinate system itself was located in the center of the dark formation at the entrance of the NLM. In (1), $L_{\mathrm{NL}} = (k|n_2|I_0)^{-1}$ is the nonlinear length, where k and n_2 stand for the wavenumber inside the NLM and the nonlinear index of refraction, respectively. In one transverse dimension ($b \to \infty$) for a certain balance intensity I_0

* *Permanent address:* Sofia University, Department of Quantum Electronics, 5, J. Bourchier Blvd., BG-1164 Sofia, Bulgaria (Fax: +35-92/962-5276, E-mail: ald@phys.uni-sofia.bg)

one has $L_{\mathrm{Diff}} = L_{\mathrm{NL}}$. The conservation of the product $I_0 a^2$ (the so-called soliton constant) is one of the criteria for identifying dark-soliton formation [5]. In the 2D case the background intensity required to achieve an OVS is $\sqrt{2}$ times as high [7, 18]. In the closest possible similarity to the pure 1D case, the slowly varying electric-field amplitude of the odd dark beam of finite length was chosen tanh-shaped

$$E(x, y) = \sqrt{I_0} B\left(r_{1,0}(x, y)\right) \times \tanh\left[r_{\alpha,\beta}(x, y)/a\right] \exp\left\{i \Phi_{\alpha,\beta}(x, y)\right\} , \qquad (2)$$

where $r_{\alpha,\beta}(x, y) = \sqrt{x^2 + \alpha(y + \beta b)^2}$ is the effective Cartesian/radial coordinate

$$\alpha = \begin{cases} 0 & \text{for} \quad |y| \le b\,, \\ 1 & \text{and} \quad \beta = -1 \quad \text{for} \quad y > b\,, \\ 1 & \text{and} \quad \beta = 1 \quad \text{for} \quad y \le -b\,. \end{cases} \qquad (3)$$

The phase distribution containing two offset phase ramps of opposite helicities separated by a phase step was modeled by

$$\Phi_{\alpha,\beta}(x, y) = -\beta \arctan\left(\frac{\alpha x}{y + b\beta}\right) + (1 - \alpha)\,\mathrm{sgn}\,(x)(\pi/2)\,. \qquad (4)$$

In Fig. 1 we present a 2D gray-scale image of the initial intensity distribution of the dark beam considered (a) and a 3D-plot of its phase portrait (b). In order to avoid any influence of the finite background beam [17] of a super-Gaussian form factor $B(r) = \exp\left\{-\left(\sqrt{x^2 + y^2}/w^2\right)^{14}\right\}$, its width was chosen to exceed at least 15 times the width of the dark stripe along the x axis.

Equation (1) was solved numerically by the split-step Fourier method over a 1024×1024 grid.

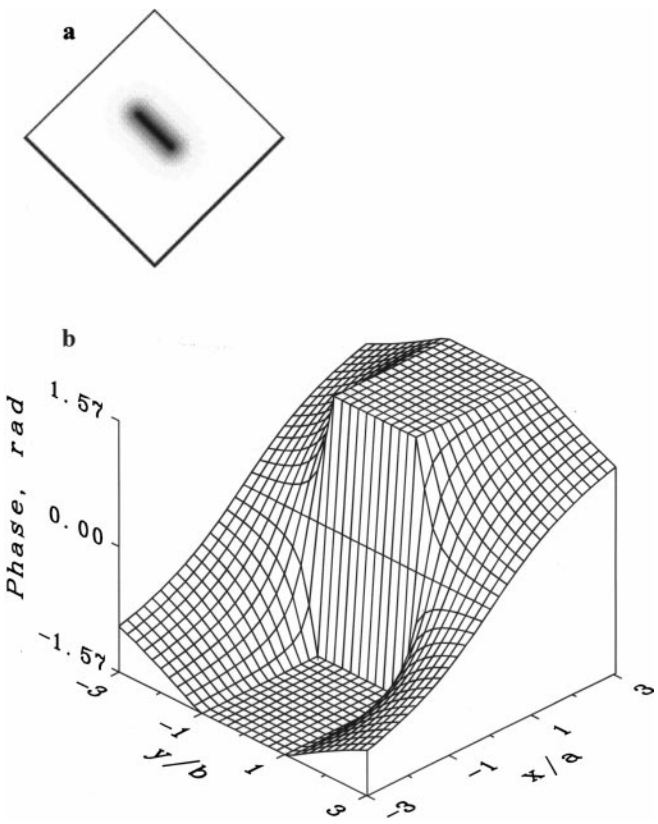

Fig. 1a,b. Qualitative intensity (**a**) and phase distribution (**b**) of the black stripe of finite length at the entrance of the nonlinear medium. The mixed edge–screw π-phase dislocation can be clearly seen

2 Results and discussion

2.1 *Soliton nature of the formation*

The asymmetry in the phase distribution (see Fig. 1b) is indicative of the differences in the evolution of the dark stripe along the transverse axes (Figs. 2–4). Although the exact one-dimensional π-phase jump implies a zero transverse velocity for an infinitely extended 1D DSS, the mixed phase dislocation causes the dark beam to steer toward the region with an initially lower phase (Fig. 2). The arrows denote three characteristic stages of evolution of the dark beam's central slice (at $y = 0$). The quantity $I_0 a^2$ was chosen equal to $\sqrt{2}$, which corresponds (at $b = a$ and a single on-axis 2π screw dislocation) to the OVS constant [7, 19]. In our case ($b/a = 2.75$) the background beam intensity was found to be overdosed, i.e. higher than suggested by the quantity $I_0 a^2$. Initially, a gray dispersive wave is emitted parallel to the edge dislocation on the higher-phase region (Fig. 3a), which results in a weak effective broadening (see Fig. 2) of the central part of the stripe. After the emission of a second dispersive wave in the opposite direction the width a of the dark stripe stabilizes and remains constant (Fig. 3c). (This second dispersive wave cannot be seen very clearly on Fig. 3b because of its low modulation depth.) The nonlinear propagation distance in this simulation was limited to $5L_{\mathrm{NL}}$ in order to get better accuracy. The mixed phase dislocation remained stable (Fig. 3c, lower row). Note that in the gray-scale phase images white and black denote phases of $-\pi/2$ and $\pi/2$, respectively.

Since a pair of opposite phase jumps on π are present in the dark-stripe slice at $x = 0$, the combined action of the

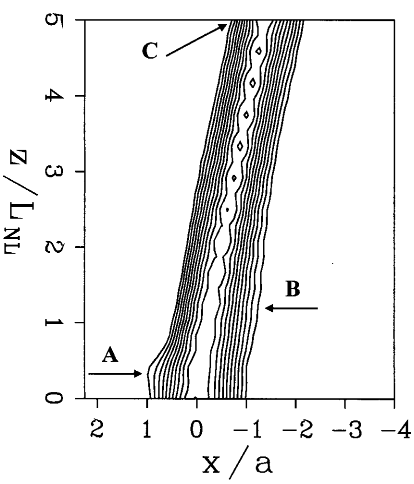

Fig. 2. Evolution of the dark beam perpendicular to the edge dislocation up to $z = 5L_{\mathrm{NL}}$ at $b/a = 2.75$. The *two outer contours* correspond to the $1/e$ intensity level of the background beam. The *arrows* indicate three characteristic evolution stages (see Fig. 3 and the text)

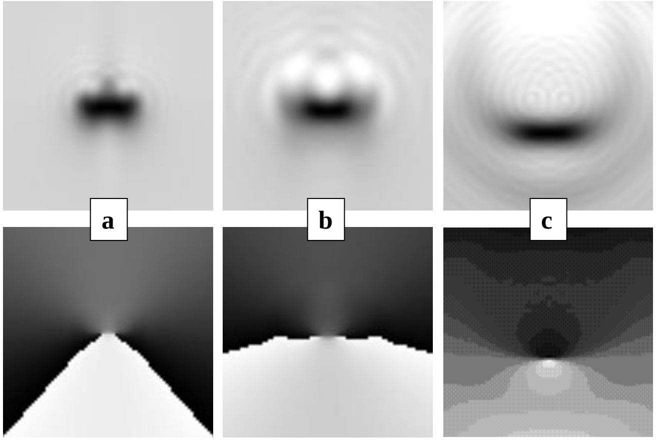

Fig. 3. Gray-scale images of the intensity (*upper row*) and phase (*lower row*) at the propagation pathlengths denoted in Fig. 2 ($I_0a^2 = 1.4$, $b/a = 2.75$)

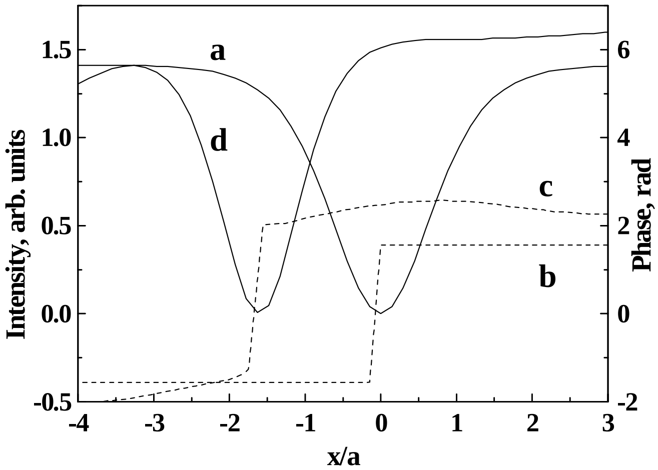

Fig. 5. One-dimensional intensity (*solid curves*) and phase (*dashed curves*) profiles of the 1D odd dark beam of finite length at $y = 0$ (*right pair*) and $z = 5L_{\mathrm{NL}}$ (*left pair*)

slight attraction between the semi-helices, the beam steering, and the weak dark-beam diffraction along the y axis (due to the strongly offset tanh-shaped dark-beam wings) leads to a monotonic increase in the stripe length (Fig. 4) at the expense of a shortening of the edge dislocation. The later was found to depend on the ratio b/a.

It is known [1, 11, 20, 21] that pairs of optical vortices of opposite topological charges translate and may collide and annihilate. In a comparative simulation we generated two OVSs of radii a and opposite topological charges (TCs) with a spatial offset of $\Delta = b = 2.75a$. In this case the semi-helices have the same spatial positions as the screw dislocations of the OVSs and the latter attracted considerably. We found that, besides the linearity vs. propagation pathlength distance, the steering velocity of the dark stripe with mixed phase dislocation is $2(\pm 0.1)$ as high as that of the OVS-pair.

For $b/a \leq 1.8$ the optical vortices collide and annihilate, whereas the stripe with mixed-type phase dislocation steers and remains topologically stable. Perpendicular to the edge dislocation (at $y = 0$) the π-phase step (Fig. 5, curve b) remains unchanged (curve c) and centered on the intensity minimum (curve d on Fig. 5, $z = 5L_{\mathrm{NL}}$). The latter reaches the zero-intensity level. The quantity $I_0a^2 = 1$ at $I_0 = \sqrt{2}$ remains conserved as a consequence of the $2^{1/4}$-fold narrowing of the stripe. Due to the non-negligible 2D intensity redistribution caused by the beam steering, the accuracy of the above estimates is within 2.5%. At $I_0 = 2.5$ a diverging gray arc of decreasing contrast is radiated, steering at approximately twice the transverse velocity of the beam with the mixed phase dislocation. In contrast, the 1D ODSSs with pure edge dislocation emit symmetric pairs of diverging gray DSSs. At a background intensity equal to that required to achieve a fundamental 1D ODSS of the same width, the width itself remains constant. The results mentioned above do not allow us to classify the formation as 1D dark spatial soliton of finite length. The steering process tends to reshape the wing of the dark beam along the y axis and the length changes slightly. In a series of additional simulations we proved that the collision of two 1D ODBs of finite and equal lengths steering in opposite directions results in annihilation of the TCs and in creation of ring dark solitary waves [14–16]. For this reason we adopt the classification '1D odd dark beam of finite length'.

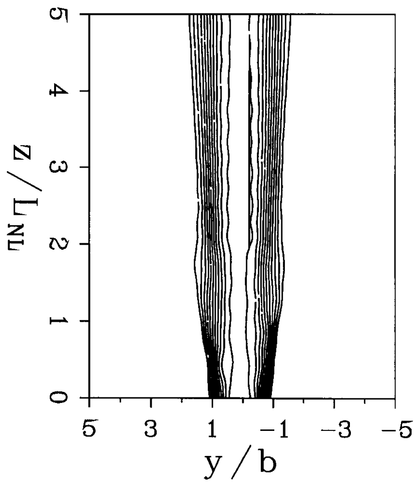

Fig. 4. Evolution of the dark beam along the edge dislocation (at $x = 0$) up to $z = 5L_{\mathrm{NL}}$ at $b/a = 2.75$. The *outer contours* correspond to the $1/e$ intensity level of the background beam

Because of the spatial steering and the interaction between the semi-helices, however, the final evolution stage of the formation should be expected to be a 'gray' one. A decrease of the contrast by up to 90% of the initial one was observed at $b/a = 1.6$ and $z = 7.5L_{\mathrm{NL}}$. Therefore, the length b of the dark stripe appears to be an important characteristic of the formation. The emission of dispersive waves in the initial stage of the soliton formation and the 2D intensity redistribution on the background may initiate modulational instability and destroy the formation. For a finite dark stripe with mixed phase dislocation initially that was much longer than it was wide ($b/a = 11$) we observed that it decayed (Fig. 6a, $z = 5L_{\mathrm{NL}}$) into a chain of optical vortices with alternating TCs. This instability scenario known for the plane dark solitons [22] is confirmed experimentally in both isotropic [23] and anisotropic [24, 25] nonlinear media. The characteristic initial slight beam expansion (Fig. 2a), bending (Fig. 3a), and emission of dispersive waves are still present at $b/a = 2.75$, but the perturbation is not critical in respect of spatial fre-

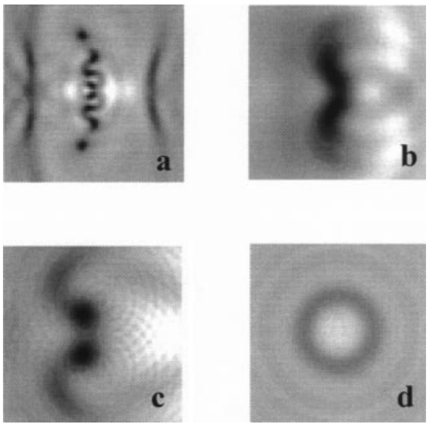

Fig. 6a–d. Final stage (**a**) of the development of snake-instability at $I_0 a^2 = 1.4$ and $b/a = 11$ at $z = 5L_{\mathrm{NL}}$. At $b/a = 4$ the dark stripe bends (**b** – at $z = 2L_{\mathrm{NL}}$) and the instability results in a pair of interacting OVSs of opposite TCs (**c** – $z = 5L_{\mathrm{NL}}$). **d** – generation of a ring dark solitary wave at $b = 0$ and $\Phi = \mathrm{const}$.

quency. The ratio $b/a = 4$ was found to be larger than the critical one and stripe bending (Fig. 6b, $z = 2.5L_{\mathrm{NL}}$) and decay in a pair of OVSs of opposite TCs (Fig. 6c, $z = 5L_{\mathrm{NL}}$) were observed. Formally, assigning a TC of $\pm 1/2$ to the semi-helices, the total TC remains conserved. In the limiting case $b = 0$ and $\Phi = \mathrm{const}$ under the same model conditions we observed the formation of a ring dark solitary wave [14] with its typical phase portrait [15], nonzero transverse velocity, and reducing contrast [14, 16] along the propagation axis (Fig. 6d).

2.2 Interaction between 1D odd dark beams of finite length

Although the ability of 1D ODSSs and OVSs to induce waveguides for signal waves has been confirmed experimentally (see, for example, [7]) and the same should hold for 1D ODBs of finite length, we will not discuss the applicability of particular short-distance all-optical switching schemes [9, 26, 27]. The dark beams described in this work can be aligned on a 'dashed' line (Fig. 7a, initial offset $\Delta y = 2b$). If the two edge dislocations have the same orientation, the neighboring semi-helices appear with opposite TCs. The latter can give rise to attraction (Fig. 7b) and the neighboring vortices can annihilate (Fig. 7c, $z = 7L_{\mathrm{NL}}$). By increasing the offset ($\Delta y = 3b$) the interaction can be effectively suppressed. Varying the mutual orientation of the edge dislocations only should make

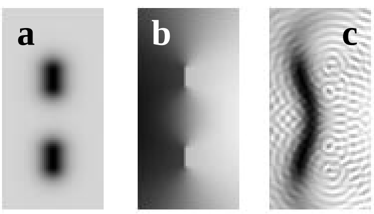

Fig. 7a–c. Side-by-side disposition of two 1D ODBs at $\Delta y = 2b$ (**a**, **b** – intensity and phase distributions, respectively; **c** – side attraction causing annihilation of the neighboring semi-vortices washing out the edge dislocations). Stabilization (up to at least $7.5L_{\mathrm{NL}}$) is found at $\Delta y = 3b$ (see Fig. 8b)

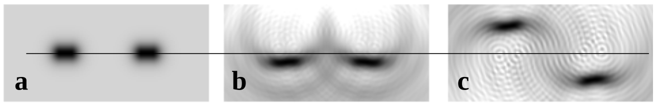

Fig. 8a–c. Controllable steering and interaction in a pair of 1D ODBs of finite length at $\Delta y = 3b$ and $z = 0$ (**a**) and $7L_{\mathrm{NL}}$ (**b**, **c**). The steering direction is controlled by changing the edge dislocations from identical phase jumps (**b**) to opposite (**c**) ones. The *dashed line* denotes the initial common axis

it possible to steer the two dark beams (Fig. 8a, $z = 7L_{\mathrm{NL}}$) in the same (Fig. 8b) or in opposite directions (Fig. 8c). When the neighboring edge dislocations carry the same 'charges', the steering angle is considerably larger (Fig. 8c). In view of the repulsive interaction between OVSs of equal TCs leading to their rotation, this could be intuitively understood by the enhanced bending of the phase lines in between. In the initial stage of the nonlinear evolution the neighboring semi-helices of equal charges of $1/2$ rotate slightly, giving rise to the dark beam steering in opposite directions. The slightly larger steering of the neighboring ends of the beams as compared with that of the outer ones supports such an interaction scenario. If an OVS is formed instead of one of the 1D ODBs considered, this could preserve (at a large enough spatial offset) its spatial position on the background. So, the switching between different initial phase profiles will enable the steering of the 1D ODBs of finite length to be controlled. Eventually, this could allow deflection of guided streams of optical information in space. The mixed edge–screw phase dislocations needed could be obtained by means of, for instance, electrically controllable, multiple active, computer-generated holograms [28]. By applying a single voltage this device could generate any wavefront out of a set of desired uncorrelated optical wavefronts [28].

3 Conclusion

In view of the above results it is worth noting that the analyzed one-dimensional odd dark beams of finite length have many features in common with OVSs and 1D ODSSs. The characteristic mixed edge–screw phase dislocation, however, forces them to steer in space and influences the interaction between such formations. Despite some of the criteria [5] for identifying a dark (asymptotically gray) spatial soliton are satisfied, we can not classify these beams as solitons in the usual sense [13]. In a previous experiment [12] we observed the creation of such mixed phase dislocations as a result of the modulational instability of crossed dark soliton stripes at moderate saturation of the nonlinearity. It is also important to study both analytically and experimentally the modulational stability of 1D ODBs of finite length, starting from controllable initial conditions (for example by reproducing computer-generated holograms), and evaluate the guiding quality of signal beams/pulses. Experimental studies on these problems are currently under preparation.

Acknowledgements. A.D. would like to thank the Alexander von Humboldt Foundation for the award of a fellowship and the opportunity to work in the stimulating atmosphere of the Max-Planck-Institut für Quantenoptik (Garching, Germany). The authors are grateful to Prof. H. Walther for his continuous interest, support, and critical appraisal of the manuscript. This work was also supported by the National Science Foundation of Bulgaria.

References

1. J.F. Nye, M.V. Berry: Proc. R. Soc. London A **336**, 165 (1974)
2. A. Hasegawa, F. Tappert: Appl. Phys. Lett. **23**, 171 (1973); V. Zakharov, A. Shabat: Sov. Phys. JETP **37**, 823 (1973), in Russian: Zh. Eksp. Th. Fiz. **64**, 1627 (1973)
3. P. Emplit, J. Hamaide, F. Reynaud, C. Froehly, A. Barthelemy: Opt. Commun. **62**, 374 (1987)
4. A. Weiner, J. Heritage, R. Hawkins, R. Thurston, E. Kirschner, D. Leaird, W. Tomlinson: Phys. Rev. Lett. **61**, 2445 (1988)
5. G. Allan, S. Skiner, D. Andersen, A. Smirl: Opt. Lett. **16**, 156 (1991)
6. G. Swartzlander Jr., D. Andersen, J. Regan, H. Yin, A. Kaplan: Phys. Rev. Lett. **66**, 1583 (1991); D. Andersen, A. Hooton, G. Swartzlander Jr., A. Kaplan: Opt. Lett. **15**, 783 (1990)
7. G. Swartzlander Jr., C. Law: Phys. Rev. Lett. **69**, 2503 (1992)
8. C. Law, G. Swartzlander Jr.: Opt. Lett. **18**, 586 (1993)
9. B. Luther-Davies, R. Powles, V. Tikhonenko: Opt. Lett. **19**, 1816 (1994)
10. V. Bazhenov, M. Soskin, M. Vasnetsov: J. Mod. Opt. **39**, 985 (1992); I. Basistiy, V. Bazhenov, M. Soskin, M. Vasnetsov: Opt. Commun. **103**, 422 (1993)
11. Y.S. Kivshar, B. Luther-Davies: Phys. Rep. **289**, 81 (1997)
12. A. Dreischuh, G.G. Paulus, F. Zacher: Appl. Phys. B **69** (1999)
13. M. Remoissenet: *Waves Called Solitons* (Springer, Berlin, Heidelberg, New York 1994)
14. Y.S. Kivshar: Phys. Rev. E **50**, R40 (1994)
15. A. Dreischuh, W. Fließer, I. Velchev, S. Dinev, L. Windholz: Appl. Phys. B **62**, 139 (1996)
16. D. Neshev, A. Dreischuh, V. Kamenov, I. Stefanov, S. Dinev, W. Fließer, L. Windholz: Appl. Phys. B **64**, 429 (1997)
17. Y.S. Kivshar, X. Yang: Opt.Commun. **107**, 93 (1994)
18. S. Balushev, A. Dreischuh, I. Velchev, S. Dinev, O. Marazov: Phys. Rev. E **52**, 5517 (1995)
19. I. Velchev, A. Dreischuh, D. Neshev, S. Dinev: Opt. Commun. **140**, 77 (1997)
20. G. Indebetouw: J. Mod. Optics **40**, 73 (1993); I. Basisty, V. Bazhenov, M. Soskin, M. Vasnetsov: Opt. Commun. **103**, 422 (1993)
21. K. Staliunas: Chaos, Solitons and Fractals **4**, 1783 (1994)
22. D. Pelinovsky, Y. Stepanyants, Y. Kivshar: Phys. Rev. E **51**, 5016 (1995)
23. V. Tikhonenko, J. Christou, B. Luther-Davies, Y.S. Kivshar: Opt. Lett. **21**, 1129 (1996)
24. A.V. Mamaev, M. Saffman, D.Z. Anderson, A.A. Zozulya: Phys. Rev. A **54**, 870 (1996)
25. A.V. Mamaev, M. Saffman, A.A. Zozulya: Phys. Rev. Lett. **76**, 2262 (1996)
26. V. Kamenov, A. Dreischuh, S. Dinev: Phys. Scr. **55**, 68 (1997)
27. A. Berzanskis, A. Matijosius, A. Piskarskas, V. Smilgevicius, A. Stabinis: Opt. Commun. **140**, 273 (1997)
28. C. Slinger, P. Brett, V. Hui, G. Monnington, D. Pain, I. Sage: Opt. Lett. **22**, 1113 (1997)